

BRAZED DISPERSION STRENGTHENED COPPER: THE EFFECT OF NEUTRON IRRADIATION AND TRANSMUTATION ON BOND INTEGRITY

D.J. Edwards^(a), F.A. Garner, M.L. Hamilton^(b), and J.D. Troxell^(c)

OBJECTIVE

The objective of this study was to investigate the effect of neutron irradiation at high temperatures on the integrity of brazed copper joints. Four different braze alloys were studied to determine their suitability for use in a neutron environment.

SUMMARY

Four types of brazes were used to join sheets of GlidCop CuAl25. Miniature tensile specimens and TEM disks were fabricated from the joints, and irradiated under various conditions to study their response to high temperature neutron irradiation. Two of the brazes, TiCuAg and TiCuNi, were eliminated from consideration because of the poor quality of the brazed joints. Brazed joints produced using a gold-containing braze were satisfactory for the unirradiated state. However, transmutation of Au to Hg affected the integrity of some of the joints in the specimens irradiated in a below-core position where the neutron spectrum was much softer. A CuAg braze yielded satisfactory joints in the unirradiated state, and held up very well when the irradiated specimens were tested. However, transmutation of Ag to Cd leads to a high residual radioactivity that limits the usefulness of this braze after exposure to neutron irradiation. Further work is necessary to identify brazes that are "transmutation-resistant" and also that minimize the potential for activation by a suitable choice of elemental constituents.

TECHNICAL PROGRESS

Introduction

The first wall and divertor structure for the ITER device require a material that can withstand both the high heat flux (5 MW/m^2) and the irradiation damage resulting from interaction with the fusion plasma. Current designs call for a beryllium or carbon fiber composite (CFC) armor bonded to a copper alloy, which in turn is joined to 316LN stainless steel. Dispersion strengthened copper (DS Cu) is currently the main candidate alloy, with the precipitation hardened alloys CuNiBe and CuCrZr being considered as the backup materials.

Past research has centered mainly upon the properties and behavior of the base materials after exposure to neutron irradiation. A new area of research that has only recently been given attention within the fusion materials community is the joining of DS copper to other materials, namely stainless steel and beryllium. A number of methods for joining copper alloys to stainless steel are

^(a)Associated Western Universities, Richland, WA 99352

^(b)Pacific Northwest Laboratory, Richland, WA 99352

^(c)SCM Metal Products, Inc., Triangle Park, NC, 27709-2166

being evaluated, including hot isostatic pressing, explosive bonding, and brazing. The bonding of copper alloys to stainless steel or beryllium to form the large, integral structures needed in ITER poses a significant technical challenge, both from the fabrication perspective and from the effect of neutron irradiation on the joints.

Of the three joining methods mentioned above, brazing appears to have several problems that need to be addressed. Most notable is the effect of transmutation on the constituents in the braze [1], as well as excessive diffusion of the braze constituents into the base material during the joining process. The latter is a problem commonly encountered when using brazes with a high silver content [2].

This study is the first effort to gain insight into the effect of neutron irradiation on brazed joints. Brazed DS copper specimens were irradiated at three different conditions in the Fast Flux Test Facility (FFTF) [3], then tested afterwards to ascertain the effect of irradiation damage and transmutation. This report summarizes the results of the mechanical testing and preliminary characterization of the joints.

Experimental Procedure

Using four different brazing alloys, sheets of LOX grade GlidCop CuAl25 were brazed together to form a lapped joint. The CuAl25 used for this experiment was in the 96% cold worked condition and nominally 0.254 mm thick. No post-braze heat treatment was applied. The compositions and brazing conditions are listed in Table 1, along with information concerning the liquidus and solidus temperatures. After brazing, the joined sheets were then shipped to a commercial vendor to have miniature lapped tensile specimens fabricated by a wire electrical discharge machining (EDM) process from the joints. The final dimensions and geometry of the specimens are illustrated in Figure 1. For comparison, tensile specimens were also fabricated by EDM from the original CuAl25 sheet in two orientations: parallel and perpendicular to the rolling direction. Excluding the joint overlap, the size and geometry of the specimens were identical to that of the brazed specimens.

Since the GlidCop alloys typically have a large grain boundary area due to the fine grain size (~1 μm wide x 5 μm long), excessive migration of the silver from the joint into the base metal occurs during brazing. Samal [2] developed a procedure to minimize such diffusion of the silver into the grain boundaries. Essentially the GlidCop surface is plated with a layer of pure copper having a grain size on the order of several microns. The smaller grain boundary area of the interface layer effectively eliminates the migration of the silver. For the CuAg and TiCuAg brazes in this experiment, CuAl25 with a 0.015 mm cladding of pure copper was used in place of plated GlidCop. The copper cladding is a remnant of the extrusion process, and normally would be machined off. In this case the pure copper cladding was left in place after the brazing, so the specimen thickness measurements include the thickness of the cladding. The specimens brazed with CuAu and TiCuNi were brazed in the declad state. Brazing time was 5 minutes, with the specimens left to cool in the furnace for ~20 minutes.

Specimens of each type of braze and of the 96% CW CuAl25 were irradiated in the Fast Flux Test Facility (FFTF) located in Richland, Washington. The specimens were irradiated at three different locations in the FFTF Materials Open Test Assembly, which lead to the specimens being irradiated at three different dose rates due to differences in the neutron spectrum at each location. The

irradiation conditions are provided in Table 2. All specimens, regardless of location, were in reactor a total of 203 effective full power days. At least three specimens of each type of material were irradiated at each set of conditions. CuAg brazed specimens were not included in the capsules irradiated to 34.5 dpa at 706 K.

The miniature specimens were tested in a specially designed horizontal testing frame used to test both nonradioactive and radioactive specimens. The specimen is held by wedge grips that have a small square grid on one half of each grip to improve the grip's ability to clamp and hold the specimen. The load on the specimen is monitored during the tightening of the grips to minimize any tensile stresses that may be incurred by clamping the specimen. All tensile tests were performed at room temperature using a strain rate of $4 \times 10^{-4} \text{s}^{-1}$.

Because of the small size and the high residual radioactivity of the irradiated specimens, the latter of which hampers the handling of the specimens, strain cannot be easily measured using strain gages. Consequently, the strain is calculated by measuring the crosshead displacement using a linear variable displacement transducer. The displacement is converted to strain by assuming that all of the deformation occurs in the gage section of the tensile specimen. Although the strain values for these miniature specimens may not be directly comparable to that obtained from full size specimens, they can be used to demonstrate any trends that may occur. However, the strength values are thought to be comparable to those measured from full size specimens [4,5].

Maximum shear stress values were calculated at the maximum load using areas measured from optical micrographs of the cross-section of each specimen tested. The joints were not uniform in shape or dimension, so in many cases the lapped area was estimated based on an average of the dimensions that could be measured readily from the optical micrographs. The shear stress values are considered to be rough estimates that might be in error by up to as much as 15%, whereas the experimental error for typical yield and UTS values lies within $\pm 5\%$. The smaller error in the yield and UTS is due to the more accurate dimensional measurements that can be obtained for the thickness and width of the gage section.

An illustration of the test configuration used for the lapped miniature tensile specimens is provided in Figure 2. Because the two specimen halves were offset, bending stresses were introduced during testing. These were minimized by placing shims in the position indicated in Figure 2. The shims were fabricated by cutting the grip ends off of extra specimens of the base material. It was initially thought that the shims might slip during the testing, but by tightening the grips sufficiently this problem did not occur. Since no adhesive was required to prevent slippage, this simplified the testing procedure and reduced both the radiation exposure to the operator and the potential for contamination.

After testing, fracture surfaces of representative specimens for each braze alloy were examined in a JEOL 840 SEM equipped with an energy dispersive spectrometer. Metallography and SEM were used to examine the polished cross-sections of the unirradiated specimens. The polished cross-sections of the joints were imaged using backscattered electrons in the SEM. Backscatter imaging reveals contrast because of atomic number differences, so that those areas containing high concentrations of silver or gold (higher atomic number than copper) appeared brighter than the surrounding areas of pure copper. Conversely, regions with significant levels of titanium or aluminum showed up darker than the surrounding matrix because their atomic numbers were lower than that of pure copper.

Results and Discussion

Of the four brazing alloys tested, the TiCuAg and TiCuNi did not produce acceptable joints. Figures 3 and 4 illustrate the poor quality of the joints produced using these alloys. Referring to the TiCuAg joints in Figure 3a, massive migration of the silver occurred from the braze into the base material over a distance of several hundred microns. A close look at the surface (Figure 3b) shows that the silver is concentrated primarily at the grain boundaries due to grain boundary diffusion. The dark regions represent porosity at the grain boundaries rather than regions high in titanium or aluminum. Some of the specimens appeared to be warped, possibly as a result of the silver diffusion and the porosity formation in the joint. All of the TiCuAg specimens tested in both the unirradiated and irradiated state failed prematurely. Surprisingly, the specimens failed outside the joint in the region where the silver had reached the limit of its migration. In contrast to the TiCuAg joints, the CuAg joints were in general quite good, although there were a few specimens that had small amounts of porosity in the joint. It is not clear why the TiCuAg joints were of such poor quality. Both the CuAg and the TiCuAg joints were formed using clad CuAl25 from the same stock. The brazing temperature for the TiCuAg was higher by ~80 K, which is the only known variable in the process and may have been responsible for the problem.

The TiCuNi joint in Figure 4a illustrates that the base metal was melted during the brazing. The resulting microstructure of the joint is rather complex, consisting of intermetallic phases and a Widmanstätten microstructure of beta and alpha titanium. A closeup of a Widmanstätten colony is shown in Figure 4b. The darker regions in the micrograph are regions that contain a high concentration of titanium. The darker the appearance, the more titanium that is present. As with the TiCuAg brazed specimens, the specimens also failed prematurely in both the unirradiated and irradiated specimens. The yield and UTS values for the TiCuNi specimens exhibited a large amount of variability because the melting that occurred in the joint produced uneven cross-sections. The specimens tended to fail in regions near the outer edge of the joint where the specimen was the thinnest.

The remaining two alloys showed the most promise judging by the quality of the joint in the unirradiated specimens. An example of a CuAu braze joint is shown in Figure 5a, again imaged using backscattered electron imaging. The CuAg joints were identical in overall appearance, although closer examination revealed a eutectic microstructure, which is to be expected considering the eutectic composition of the braze. An example of the eutectic microstructure is shown in Figure 5b.

The tensile data for the unirradiated and irradiated specimens of the base CuAl25 (perpendicular and parallel) and the CuAg and CuAu brazed specimens are listed in Tables 3 through 6. All of the unirradiated specimens of CuAu and CuAg failed in the base metal, not in the joint. The data for TiCuAg and the TiCuNi were not included since the specimens failed prematurely and produced data with significant scatter. Representative tensile curves for the CuAu brazed specimens and base CuAl25 (parallel orientation) are provided in Figure 6. Several things bear mentioning with respect to these curves and the tabulated data.

All of the brazed specimens, unirradiated and irradiated, exhibited a noticeable change in the slope of what corresponded to the elastic region in the standard CuAl25 specimens. While this could certainly result from a change in the elastic modulus due to the presence of the braze, it was observed after the tensile tests that the joint alignment had changed in all of the brazed specimens, i.e., the joint rotated during the test such that the lap was actually at an angle to the tensile axis.

This means that the shift in the slope of the elastic region is most likely due to the realignment of the joint. The cause of this realignment is thought to be a combination of the thinness of the specimens and the lack of constraint, but further tests and/or finite element analysis are necessary to be certain. Special care was taken to ensure that the shims were of the same thickness as the base material, and that the specimens were correctly aligned within the grips. However, this could still allow a slight misalignment since the braze filler material would add to the overall thickness of the specimen, and this would not be compensated for by the use of shims.

While it might appear that a change in elastic modulus due to the braze could also have led to such changes as were observed in the initial portion of the tensile curve, the 30 at% Au expected to transmute to Hg during irradiation below-core [3] would be expected to cause further changes; since no additional change in the initial portion of the curve was observed following irradiation, the implication is that a change in modulus is probably not responsible for the change in the curve. Void swelling could also lead to additional dimensional changes that might affect not only the alignment of the specimen but also the performance of the braze joint. The change in the slope of the elastic region, for both the unirradiated and the irradiated specimens, leads to the determination of artificially low yield strengths than would otherwise be measured. As such, these data can only be used for comparative purposes to examine trends in material behavior.

The strength of the unirradiated CuAu brazed specimens was much lower than that of the base CuAl25. Note that brazing at 1253 K for 5 minutes, followed by a 20 minute furnace cool, caused the UTS to drop roughly 150 MPa. This suggests that the brazing exposure can lead to a decrease in the strength of the base material. Somewhat surprisingly, it was found that irradiating at temperatures ranging from 643 to 706 K for ~200 days did not produce any further changes in strength beyond that already attributed to the brazing cycle. In a separate study on the tensile properties of the irradiated base CuAl25 [6], it was found similarly that the changes in the strength of the alloy were independent of the dose, displacement rate, and temperature. It was also found that the decrease in strength due to neutron irradiation under the same conditions as used in this study was the same as that incurred in the brazed materials due to the thermal exposure during brazing. It is a little unusual that the relatively short thermal exposure during brazing would produce the same effect as neutron irradiation at 643 to 706 K for ~200 days. One possible explanation is that the initial 96% cold worked state of the base CuAl25 leaves the material very susceptible to recovery and recrystallization during short high temperature exposures and the longer term neutron irradiation at lower temperatures.

As shown in Figure 7, the CuAg brazed specimens behaved essentially the same as their CuAu brazed counterparts, with one important difference. Both types of specimens exhibited a change in the slope of the initial portion of the curve. However, for reasons unknown, this effect was much more prominent in the irradiated than in the unirradiated CuAg brazed specimens. Referring to the tensile curves of the irradiated CuAg brazed specimens, the change in slope is even more significant after irradiation. The change in slope was consistent throughout each set of specimens, so it is believed to be real. One possible explanation for this difference between the unirradiated and irradiated CuAg brazed specimens is that transmutation may have had an effect. For the below-core position in the FFTF/MOTA, Garner and coworkers [3] made calculations that showed that approximately 30 at% of the Au and 20 at% of the Ag will transmute to Hg and Cd, respectively. The transmutation rates are higher in the below-core positions because of the softer neutron spectra. For the in-core positions the transmutation levels drop to ~6 at% for both Au and Ag. Although the dpa level in-core is higher, the transmutation level is still considerably lower than below the core. It is not clear whether the presence of a significant amount of Cd would

affect the elastic modulus of the CuAg brazed specimens enough to account for the observed behavior.

In the case of the CuAu brazed specimens irradiated to 5.8 dpa in the capsule located below-core, 30% transmutation of the Au led to failure in the brazed joint. An example of the fracture surface for an irradiated specimen is provided in Figure 8. The CuAu specimen failed in the joint by intergranular failure in some areas (Figure 8b), and by what looks like delamination over the rest of the surface. It is thought that Hg may have segregated to the grain boundaries, but transmission electron microscopy (TEM) will be necessary to confirm this. All of the tested CuAu brazed specimens that were irradiated to 5.8 dpa at 643 K failed in the joint, whereas the similarly irradiated CuAg brazed specimens failed in the base material. There were a few other random failures in the joints for both CuAg and CuAu brazed specimens, but these are attributed to pre-existing defects in the joint rather than transmutation.

The shear strengths calculated for these specimens (Tables 3-6) show that in every case the maximum shear stress was much lower than the uniaxial tensile yield stress, due the size of the overlap. Since the shear stress on the joint was less than the tensile stress applied outside the joint, it is not surprising that the specimens failed outside the joint in those cases where transmutation did not cause the joint to deteriorate. Subsequent experiments will need to investigate specimens with a wide range of overlap distances in the joint to establish what the minimum overlap should be before placing more specimens in reactor.

The higher transmutation rate that will occur in reactors with a softer neutron spectrum than FFTF requires that caution be exercised when irradiating brazed specimens. The level of transmutation will be much larger in mixed spectrum reactors compared to the level expected in a fusion spectrum, which must be taken into account when setting up and analyzing the data from an irradiation experiment.

The residual radioactivity of the specimens is also important in selecting a suitable braze alloy, particularly for those brazes containing significant amounts of Ag. Ag activates strongly [1], much more than the base copper or any of the other elements used in these brazes. Ti is a low activation material, so being able to use a Ti braze would be beneficial from an activation standpoint. However, as this study showed, more effort must be devoted to optimizing the brazing conditions to improve the ductility and performance of the TiCuNi braze. Au is a relatively low activation material but the formation of Hg limits its usefulness to either very low doses, or to cases where the starting level of Au in the braze can be reduced. It might be possible to use a CuAu braze containing 25 wt% Au as opposed to 50 wt%, and to use brazed components only for low dose applications within ITER.

Conclusions

None of the brazes used in this study appear to be particularly well suited for use in a fusion environment. The transmutation of Au to Hg has a detrimental affect on the integrity of the joint. Transmutation of Ag to Cd may not be as detrimental to the properties of the braze, but the high activation due to Cd formation is a significant drawback. The TiCuAg braze also contains enough Ag to limit its usefulness due to activation considerations. The poor quality of the TiCuAg braze joints produced in this study demonstrates the importance of controlling the diffusion of the Ag into the base material. The TiCuNi braze is well suited from an activation standpoint, and perhaps

further work to improve the properties of the joint will increase its suitability. The apparent melting of the base material may pose a problem, particularly if the oxide dispersion was altered to the extent that the swelling resistance was lowered.

FUTURE WORK

The brazed TEM disks, or "sandwiches", included in this experiment will be selectively examined to investigate the possible influence of the transmutation of Au and Ag, as well as search for evidence of void swelling in the joint. Further tensile tests may be conducted to determine the exact nature of the change in elasticity of the brazed specimens.

REFERENCES

1. F.A. Garner, L.R. Greenwood, and D.J. Edwards, "Transmutation in Copper-Based Brazing Materials", DOE/ER 0313-16, (1994), p. 47.
2. P. Samal, "Brazing and Diffusion Bonding of GlidCop Dispersion Strengthened Copper", *SCM Metal Products, INC. internal report*.
3. F.A. Garner and M.L. Hamilton, D.J. Edwards, B.N. Singh, J.F. Stubbins, T. Shikama, S.J. Zinkle, P. Samal, "Status of Copper Irradiation Experiments", DOE/ER 0313-10, (1991), p. 186.
4. F.A. Garner, M.L. Hamilton, H.L. Heinisch, and A.S. Kumar, "Application of Miniature Tension Specimens to Studies of Radiation Damage in Metals", ASTM STP 1204, W.R. Corwin, F.M. Haggag, and W.L. Server, Eds., American Society for Testing and Materials, Philadelphia, 1993, pp. 336-355.
5. M.L. Hamilton, M.A. Blotter, and D.J. Edwards, "Evaluation of Miniature Tension Specimen Fabrication techniques and Performance", ASTM STP 1204, W.R. Corwin, F.M. Haggag, and W.L. Server, Eds., American Society for Testing and Materials, Philadelphia, 1993, pp. 368-385.
6. D. J. Edwards, F.A. Garner, M.L. Hamilton, P. Samal, and J.D. Troxell, "High Temperature Stability of Dispersion Strengthened Copper Alloys Irradiated with Fast Neutrons", Fusion Materials Semiannual Progress Report, *this publication*.

TABLE 1. Compositions and Brazing Conditions

	AgCu	AuCu	TiCuAg	TiCuNi
Composition, wt%	72 Ag 28 Cu	50 Au 50 Cu	5.2 Ti 26.9 Cu 67.9 Ag	69.6 Ti 15.1 Cu 15.3 Ni
Brazing temp.	1069 K	1253 K	1143 K	1253 K
Protective atmosphere	H ₂ atmosphere	H ₂ atmosphere	vacuum	vacuum
Liquidus	Eutectic composition	1243 K	1123 K	1233 K
Solidus		1228 K	1103 K	1183 K

TABLE 2. Irradiation Conditions in the FFTF/MOTA Experiment

Alloy	Irradiation Temperature (K)	Fluence (E>0.1 MeV)	Total displacement (dpa)	Displacement rate (dpa/sec)
CuAg, CuAu, TiCuNi, TiCuAg Base CuAl25	643	1.14×10^{22}	5.8	3.3×10^{-7}
CuAg, CuAu, TiCuNi, TiCuAg Base CuAl25	666	3.3×10^{22}	18.4	1.1×10^{-6}
CuAu, TiCuNi, TiCuAg Base CuAl25	706	6.0×10^{22}	34.5	2.0×10^{-6}

TABLE 3. Mechanical Properties for Unirradiated Base CuAl25 and CuAg and CuAu Brazed Specimens

Braze	YS (MPa)	UTS (MPa)	Shear Strength (MPa)	UE (%)	TE (%)	Failed in joint?
CuAg	248	457	176	6.2	10.4	No
	243	458	197	5.4	9.8	No
	225	455	182	5.7	10.1	No
CuAu	237	453	241	5.9	12.1	No
	218	448	267	5.5	6.1	No
	230	449	306	5.5	11.3	No
Base CuAl25 Parallel	498	604		1.9	8.3	
	459	607		2.3	9.9	
	468	602		2.2	10.5	
Base CuAl25 Perpendicular	454	603		2.1	10.3	
	429	600		2.4	8.5	
	435	600		2.2	9.0	

TABLE 4. Mechanical Properties for Base CuAl25 and CuAg and CuAu Brazed Specimens Irradiated to 5.8 dpa at 643 K

Braze	YS (MPa)	UTS (MPa)	Shear Strength (MPa)	UE (%)	TE (%)	Failed in joint?
CuAg	227	462	144	7.7	12.1	No
	217	460	161	6.7	10.2	No
	209	429	175	7.6	12.1	No
CuAu	224	341	96	1.0	2.3	Yes
	205	303	85	-----	2.6	Yes
	214	311	76	1.0	2.2	Yes
Base CuAl25 Parallel	423	477		8.3	16.0	
	420	465		7.8	14.6	
Base CuAl25 Perpendicular	425	471		8.0	16.1	
	417	466		7.4	14.8	

TABLE 5. Mechanical Properties for Base CuAl25 and CuAg and CuAu Brazed Specimens Irradiated to 18.4 dpa at 663 K

Braze	YS (MPa)	UTS (MPa)	Shear Strength (MPa)	%UE	%TE	Failed in joint?
CuAg	186	457	119	8.4	12.7	No
	193	416	158	3.1	3.3	Yes
	181	458	161	10.3	14.7	No
CuAu	211	451	113	6.8	10.2	No
	230	435	178	6.3	8.8	No
	242	443	120	5.9	8.4	No
Base CuAl25-Parallel	389	433		8.3	15	
	419	458		7.8	19.4	
Base CuAl25-Perpendicular	407	449		8.0	18.6	
	385	450		7.4	18.5	

TABLE 6. Mechanical Properties for Base CuAl25 and CuAg and CuAu Brazed Specimens Irradiated to 34.5 dpa at 706 K

Braze	YS (MPa)	UTS (MPa)	Shear Strength (MPa)	%UE	%TE	Failed in joint?
CuAg						
CuAu	231	451	115	-----	3.6	Yes
	207	456	144	7.5	13.1	No
	224	446	116	6.7	9.5	No
Base CuAl25-Parallel	405	405		10.2	19.6	
	391	447		10.6	19.1	
Base CuAl25-Perpendicular	409	452		9.8	18.3	

Figure 1. Geometry of miniature lapped tensile specimens.

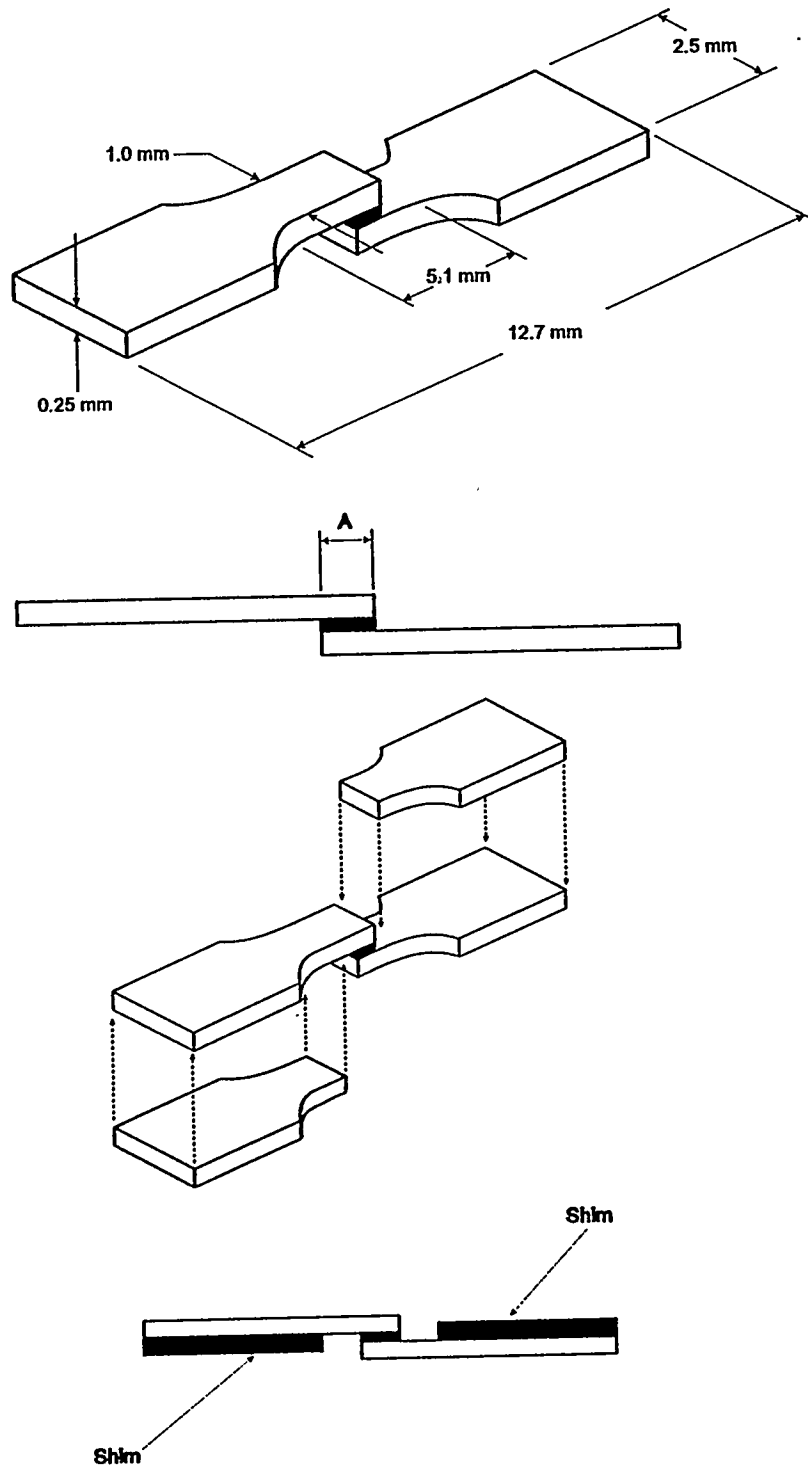


Figure 2. Use of shims during the testing to maintain the uniaxial testing condition.

Figure 3. Poor quality TiCuAg braze joint due to silver diffusion out of the joint and into the base metal.

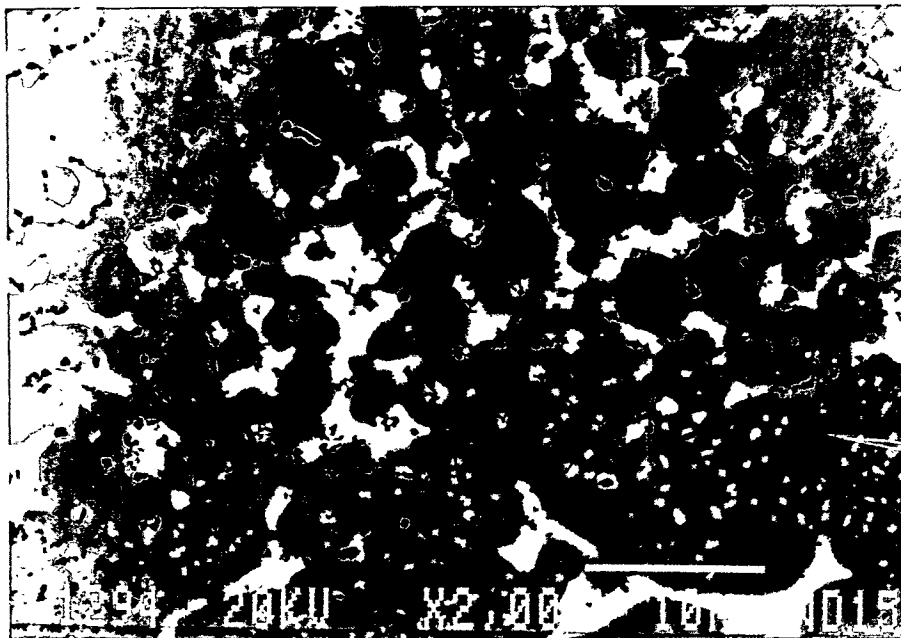
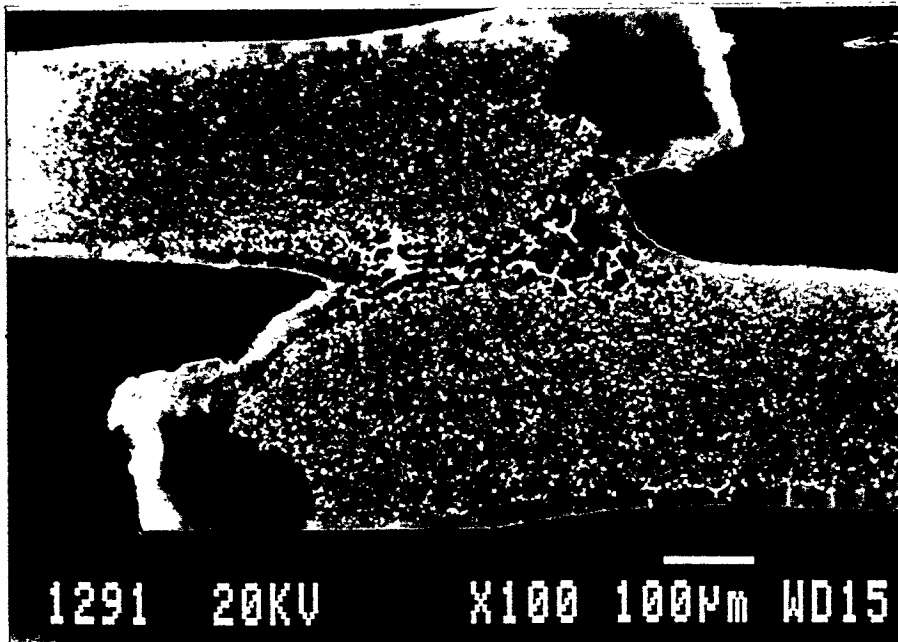


Figure 4. Melted base material and Widmanstatten structure in the TiCuNi brazed joint

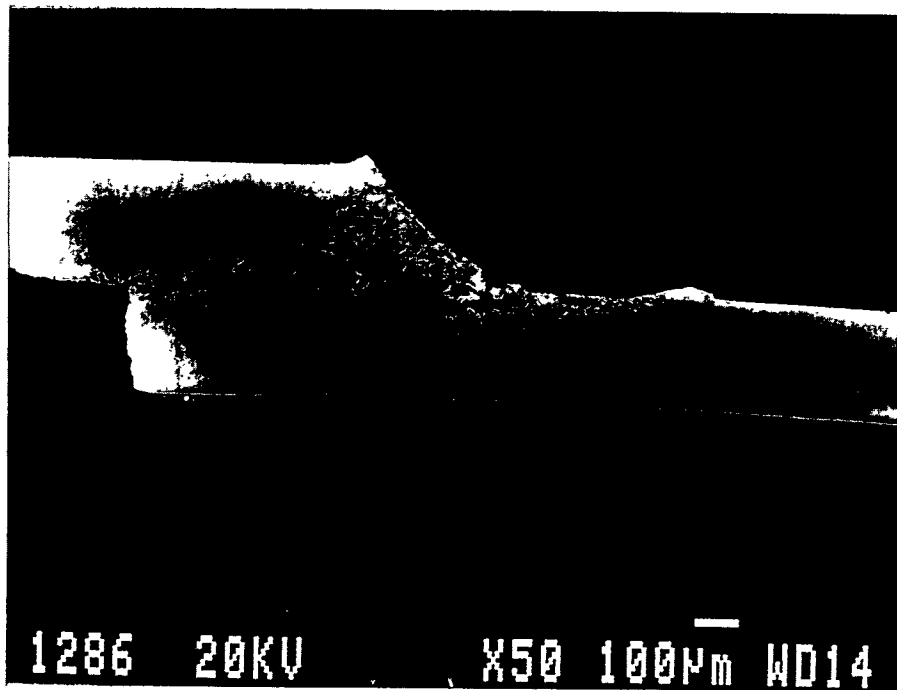
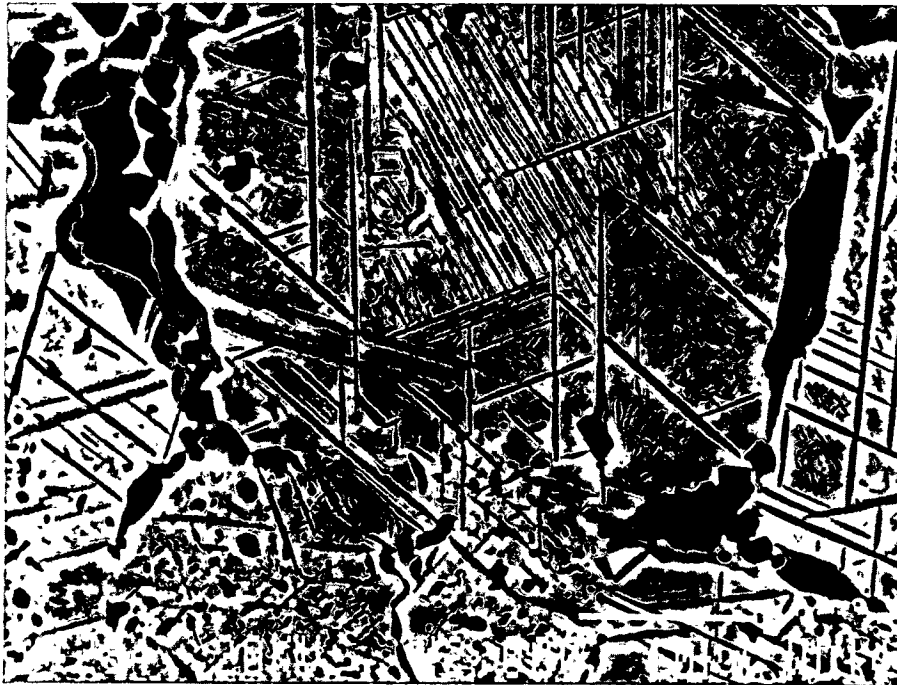


Figure 5. (a) Typical joint in a specimen containing a CuAu braze.

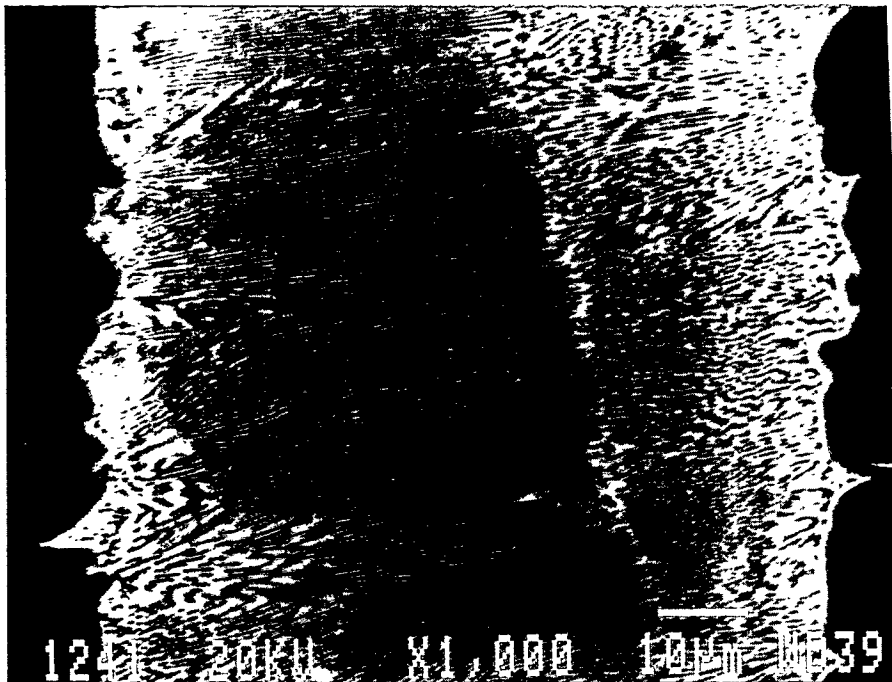
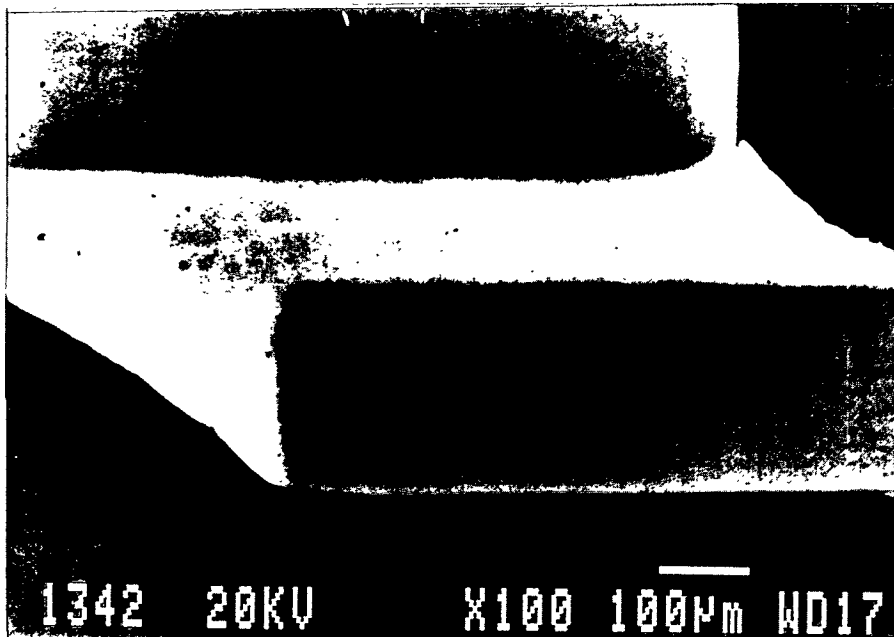


Figure 5. (b) Eutectic microstructure of the CuAg braze.

Figure 6. Tensile curves for the CuAu brazed specimens in the unirradiated and irradiated conditions, as well as the unirradiated base CuAl25 used for comparison.

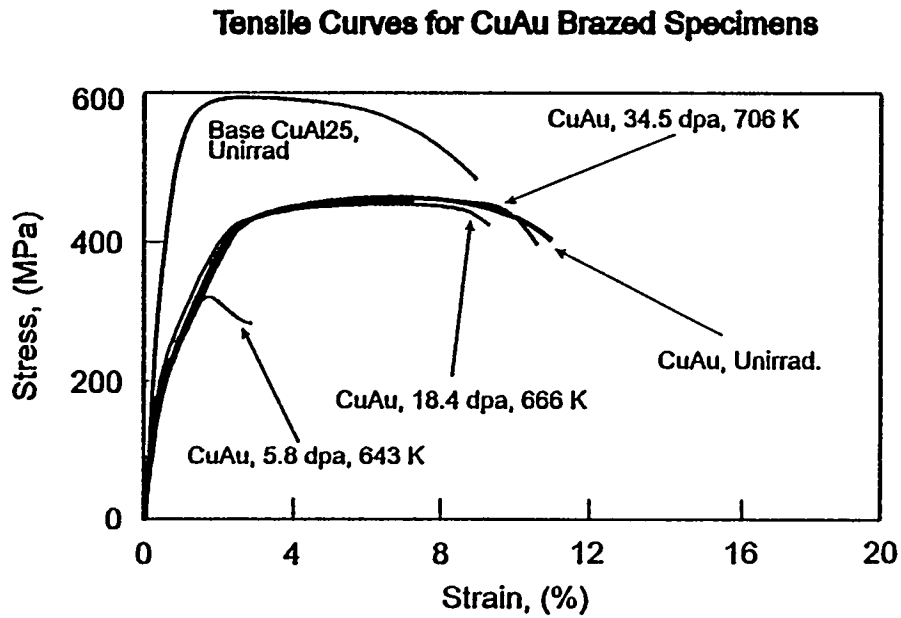


Figure 7. Tensile curves of CuAg brazed specimens in the unirradiated and irradiated conditions, as well as the unirradiated base CuAl25 used for comparison.

Figure 8. Fracture surface of the CuAu brazed specimen that failed in the joint, possibly because mercury segregated to the grain boundaries.

